Invited Paper

Comparison of Fe/Al_2O_3 and $Fe,Co/Al_2O_3$ catalysts used for production of carbon nanotubes from acetylene by CCVD

Zoltán Kónya[1*], István Vesselényi[1], Károly Lázár[2], János Kiss[3] and Imre Kiricsi[1]

[1]Applied and Environmental Chemistry Department, University of Szeged, H-6720 Szeged, Rerrich Béla tér 1, Hungary
[2]Chemical Research Center of Hungarian Academy of Sciences, Institute of Isotope and Surface Chemistry, Budapest, P.O.B. 77, H-1525, Hungary
[3]Reaction Kinetics Research Group of the Hungarian Academy of Sciences, University of Szeged, H-6701 Szeged, P.O.Box 168, Hungary

ABSTRACT

Characterization of iron containing alumina supported catalysts was performed by TEM, Mössbauer and XPS spectroscopy during formation of multiwall carbon nanotubes from acetylene at 1000 K. TEM images showed that carbon fibers (outer diameter is around 20-40 nm) were generated on Fe/Al_2O_3 samples while on the bimetallic $Fe,Co/Al_2O_3$ carbon nanotubes with an average diameter of 8-12 nm were formed. XPS spectra revealed that Fe-Co alloy formed during the interaction of $Fe,Co/Al_2O_3$ and acetylene at 1000 K. The formation of the bimetallic alloy was proven by Mössbauer spectroscopy as well.
Keywords: iron containing alumina supported catalyst, nanotubes, Mössbauer spectroscopy, XPS spectroscopy

1. INTRODUCTION

Since their discovery in 1991[1], carbon nanotubes are generating a continuously growing interest since these hollow nanostructures have exceptional electrical[2] and mechanical[3] properties making them usable in many fields. Various production methods have been developed aiming at the production of carbon nanotubes in large scale. Of the main synthetic processes, laser vaporization[4], electric arc discharge[5] and catalytic chemical deposition of hydrocarbons over metal catalysts (CCVD technique)[6], only the latter method supplies carbon nanotubes in high yield at a low cost of production. Being a catalytic process, the combinations of transition metals and supports can be changed depending on the characteristics required, for example the alignment[7] or the size of the tubes[8,9]. On the other hand, It has been demonstrated that supported transition metals (in particular iron, cobalt and nickel) on silica[10], alumina[11], zeolite- and clay-derived[12] supports are used frequently in this process[13]. For characterizing and comparing the productivity of catalysts the amount of produced carbon can be related to the amount of pristine catalyst[13]. Beside the amount of the product, the quality of carbon tubes should also be evaluated, mostly transmission electron microscopy (TEM) is used for this. In addition, as an indirect method, thermogravimetry (TG) can also be used; since the ignition temperature of amorphous carbon (the primary by-product) is smaller than that of the graphitic carbon (from which the walls of MWNTs are formed)[14].

Iron-base catalysts usually produce carbonaceous tubes with high efficiency. However, as high resolution electron microscopy studies reveal, the MWNTs may be covered with amorphous carbon in significant extents, i.e. the product is not always pure MWNT. To improve the catalyst performances, supported bimetallic systems composed from Fe, Co and Ni (2.5 wt % each) were also prepared and evaluated. Fe-Co systems were found to produce MWNTs with superior quality and yields on various supports (alumina, 13X and ZSM-5 zeolites)[15], or on mixtures of them (silica-aluminas)[16].

In the present study, for interpreting the advantageous effect of alloying Fe with Co, a report is given on the characterization of the alumina supported fresh and spent Fe-, and Fe,Co-catalysts. Samples were analyzed by Mössbauer- and infrared (IR) spectroscopies, XPS and X-ray diffraction (XRD). The formed carbonaceous products were characterized by TEM and TG techniques, as well.

Nanotechnology, Robert Vajtai, Xavier Aymerich, Laszlo B. Kish, Angel Rubio, Editors, Proceedings of SPIE Vol. 5118 (2003) © 2003 SPIE · 0277-786X/03/$15.00

2. EXPERIMENTAL

2.1 Catalysts and reaction

Preparation of the catalysts is described in detail in a previous report[16]. Briefly, the alumina prepared from aluminum isopropoxide, was impregnated with iron(II)-acetate solution containing iron in an appropriate concentration to obtain catalyst with 2.5% iron content. The bimetallic sample was prepared similarly using cobalt(II)-acetate and iron(II)-acetate solutions. The sum of metal content was 5 w%.

Catalysts were layered on a quartz boat and placed into a horizontal tubular reactor. Preceding the reaction of acetylene, catalysts were treated in nitrogen flow at 473 K, for 1 h followed by heating to the reaction temperature. At 1000 K the nitrogen flow was switched for nitrogen-acetylene gas mixture to start the CCVD reaction. After 30 min the acetylene was stopped and the catalyst was cooled to ambient temperature while nitrogen was flushing the reactor. Then the mixture of the catalyst and the product was transferred to a dry box with exclusion of air. In the dry box the mixture was impregnated with molten wax. After solidifying the sample a wafer was obtained in which the metal particles were isolated from air providing thereby semi *in situ* conditions for the further characterization.

2.2 XRD measurements

X-ray diffraction patterns were obtained on a DRON 3 diffractometer operated under computer control. XRD profiles were registered in the 3-60 2Θ range using Cu K_α radiation.

2.3 IR measurements

For IR spectroscopic study the KBr matrix wafer technique was applied. 1 mg of sample from the different stages of treatments was mixed with 100 mg KBr of spectroscopic purity. Pellets were pressed from the mixtures and their spectra were recorded with Mattson Genesis 1 FTIR spectrometer.

2.4 Thermal analysis

Thermal behavior of the catalyst samples used for production of carbon nanotubes were tested using a MOM Derivatograph Q instrument. TG-DTG-DTA features were recorded in the 300-1300 K temperature range. 100 mg of sample was placed into a ceramic sample holder and tested while the temperature was increased from ambient temperature to 1300 K in a ramp of 10 degree per min.

2.5 Mössbauer spectroscopy

Mössbauer spectra were recorded on a KFKI spectrometer in constant acceleration mode at ambient and 77 K (liquid nitrogen) temperatures. Positional parameters are related to metallic α-iron, their estimated accuracy is ±0.03 mm/s. The characteristic Mössbauer parameters were determined by decomposing the spectra to Lorentzian lines.

2.6 XPS spectroscopy

The XPS experiments were performed in an ultra-high vacuum system with a background pressure of 10^{-9} mbar, produced by an iongetter pump. The photoelectrons generated by Al K_α primary radiation (15 kV, 15 mA) were analysed with a hemispherical electron energy analyser (Kratos XSAM 800). The pass energy was set to 40 eV. An energy step width of 50 meV and a dwell time of 300 ms were used. Typically 10 scans were accumulated for each spectrum. Fitting and deconvolution of the spectra were performed with the help of VISION software. All binding energies were referenced to Al(2p) at 74.7 eV.

Before measurements, the sample was evacuated at 300 K and calcined at 1000 K for 20 min in the sample preparation chamber, which was connected directly to the analysing chamber by a sample transfer system. In the sample preparation chamber the catalyst can be heated up to 1100 K in various gas atmospheres (in the present case in acetylene-nitrogen mixture).

2.7 TEM measurements

Approximately 1 mg of product was homogenized in 10 ml ethanol for 30 min using ultrasonic treatment. A few drops of the resulting suspension were put on a carbon film coated TEM grid. TEM images were taken by a Philips CM 20 electron microscope.

3. RESULTS AND DISCUSSION

3.1 Infrared spectroscopy

The IR spectra of catalysts treated in nitrogen at 1000 K show no band due to decomposition residues of acetate salts. The reaction of catalyst in acetylene stream gives rise bands neither due to surface OH groups nor to CH residues. This reveals that product contains exclusively high purity carbon and not carbonaceous compounds having hydrogen. (More precisely, the concentration of CH groups falls below the detection limit of IR spectroscopy).

3.2 Thermogravimetry

Derivatographic patterns for the fresh and the spent catalysts samples are seen in Figure 1. The TG and DTG curves of starting specimens show three weight loss steps both for the iron and for the cobalt-iron materials. Both the temperatures and the weight losses due to the respective steps are very similar. The values are listed in Table 1.

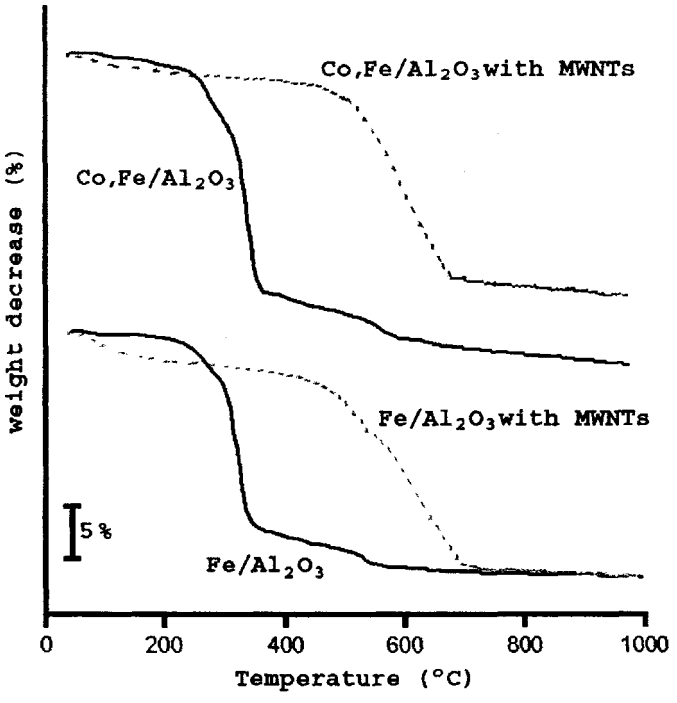

Figure 1: Derivatographic patterns of the catalysts before and after reaction

Table 1: Summary of the results obtained by derivatography.

Fe-AlOH (fresh)		Fe-AlOH (spent)	
Temperature (°C)	Weight loss (w%)	Temperature (°C)	Weight loss (w%)
248	4.3	164	4.6
327	22.5	443	
515	4.6	591	28

Co,Fe-AlOH (fresh)		Co,Fe-AlOH (spent)	
Temperature (°C)	Weight loss (w%)	Temperature (°C)	Weight loss (w%)
248	7,5	145	3
324	27,5	606	25
520	6	700	1.5

3.3 X-ray diffraction

No peaks are shown in the XRD pattern in the 3-50 2Θ range of the Fe-AlOH sample treated at 1000 K in pure nitrogen atmosphere. In contrast, the bimetallic sample treated identically exhibits a rather sharp peak at 42 2Θ in the diffractogram. XRD profiles registered with the samples operated as catalysts for carbon nanotube production show several changes compared to the simple heat treated reference samples. First, broad signals due to the carbon nanotubes are seen at 23-25 2Θ. For Fe-AlOH sample a second broad reflection appears at 45.2 2Θ. On the feature of bimetallic specimen no signal is seen in this region. The reflection additional to the signal of nanotubes is situating at the same place as for the heat treated sample, however, its intensity is much smaller. Figure 2 shows the XRD patterns of samples in the discussed regions.

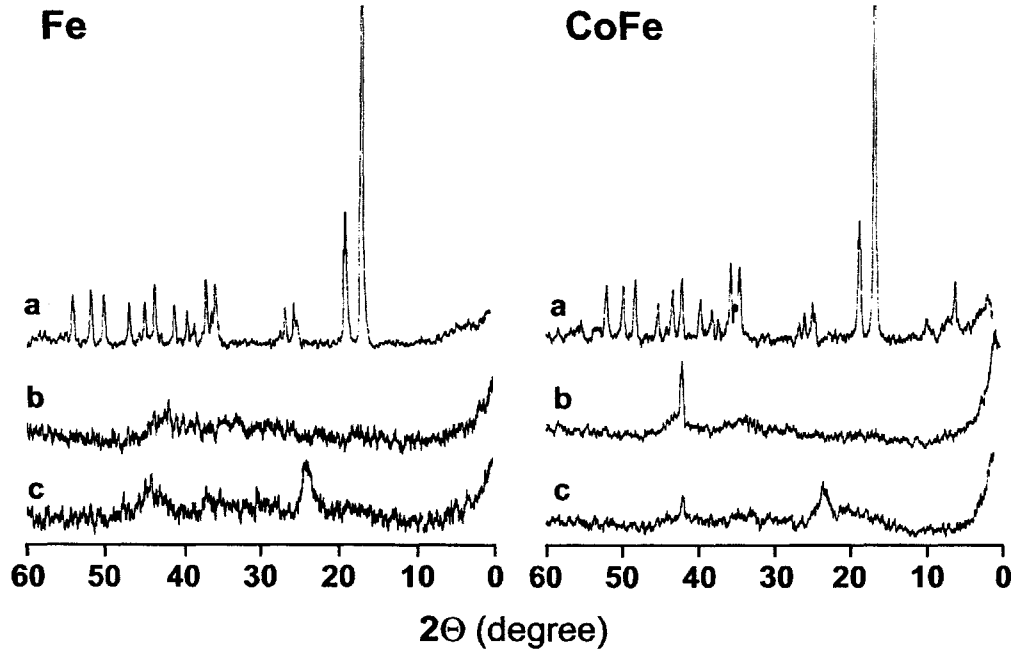

Figure 2: XRD spectra of the monometallic and the bimetallic catalysts; (a) after impregnation, (b) after calcinations in air and (c) after reaction with acetylene

3.4 CCVD reaction

Comparison of the productivity of the two catalyst showed that acetylene decomposed on both samples. However, the quality of carbon formed on the catalyst specimens was different. Carbon formed on the Fe/Al_2O_3 sample was mostly amorphous. In contrast, carbon produced on the bimetallic sample contained carbon nanotubes in rather high concentration. This present observation is in complete accordance with the literature data[17].

3.5 Characterization by TEM

The product of acetylene decomposition on Fe/Al_2O_3 showed pure carbon deposit and the carbon nanotube content was rather low, i.e. only few carbon nanotubes were found. Contrary to this, MWNTs were dominated in the deposit formed on $Co,Fe/Al_2O_3$ catalyst. Here much less amorphous carbon was detected. Two characteristic TEM images are seen in Figure 3.

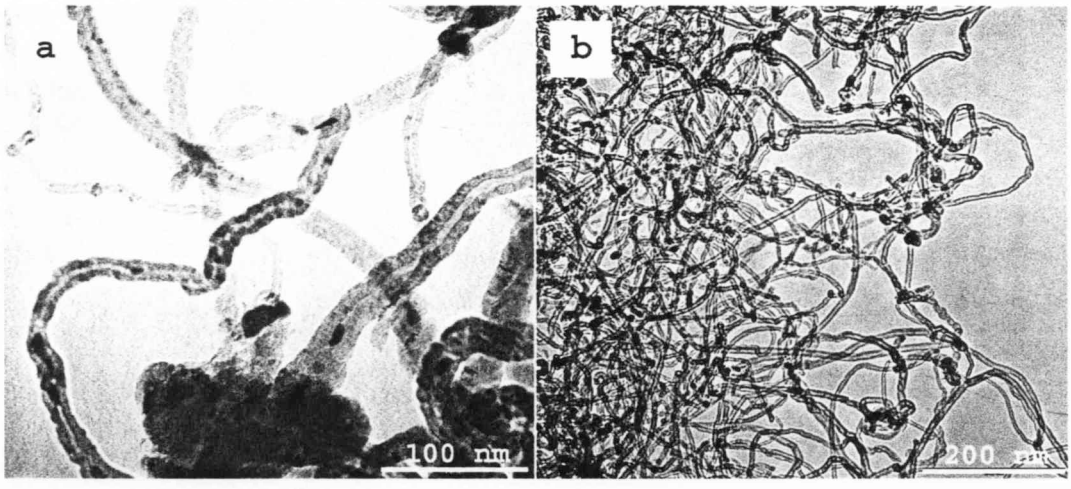

Figure 3: TEM images of fibers/nanotubes produced on Fe/Al_2O_3 (a) or $Fe,Co/Al_2O_3$ (b)

3.6 Mössbauer spectroscopy

Mössbauer spectra were recorded in two velocity ranges: ±12 and ±8 mm/s. The spectra of the wider velocity scale clearly demonstrate the transformation of the starting oxide to zerovalent metallic/carbidic components as a result of exposure to acetylene during CCVD (Fig. 4). Spectra of converted catalysts were obtained both at ambient and 77 K temperatures (Fig. 5). Data extracted from the spectra are compiled in Table 2.

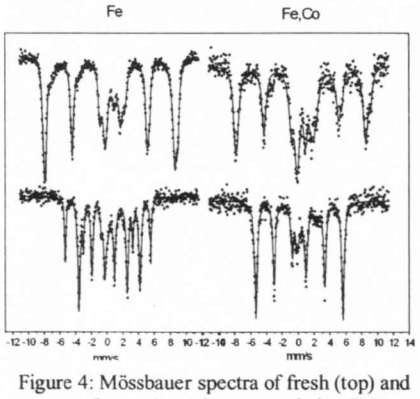

Figure 4: Mössbauer spectra of fresh (top) and spent (bottom) catalysts recorded at 77 K

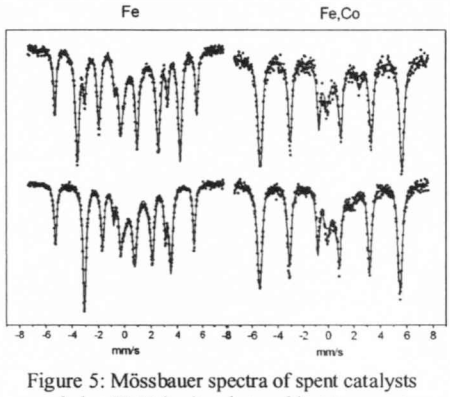

Figure 5: Mössbauer spectra of spent catalysts recorded at 77 K (top) and at ambient temperature

Table 2: Data extracted from Mössbauer spectra of fresh and spent catalysts (IS: isomer shift, relative to metallic α-iron, mm/s; QS: quadrupole splitting, mm/s; MHF: internal magnetic hyperfine field, Tesla; RI: spectral contribution, %)

Sample		Fe/Al_2O_3				$Fe,Co/Al_2O_3$			
	Comp.	IS	QS	MHF	RI	IS	QS	MHF	RI
Fresh	Fe^{3+} (A)	0.38	-	50.9	28	0.41	-	50.5	36
(77 K)	Fe^{3+} [B]	0.46	-	52.7	30	0.58	-	53.3	14
	$Fe^{(2+)3+}_{mix}$	0.76	-	47.3	16	0.53	-	43.6	14
	Fe^{3+}	0.41	1.09	-	13	0.44	1.04	-	17
	Fe^{2+}	1.04	2.52	-	12	1.02	2.38	-	19
Spent	Fe_{metal}	0.12	-	33.8	24	0.14	-	33.6	19
(77 K)	$FeCo_{alloy}$					0.14	-	34.5	62
	Θ-Fe_3C	0.32	-	24.3	58				
	$Fe^{2+/3+}$	0.79	1.29	-	9				
	Fe^{2+}	1.16	2.54	-	8	1.16	2.51		10
	Fe^{3+}					0.35	0.76	-	9
Spent	Fe_{metal}	0.02	-	33.0	29	0.04	-	33.4	27
(300 K)	$FeCo_{alloy}$					0.03	-	34.3	51
	Θ-Fe_3C	0.21	-	20.4	49			-	
	Fe^{2+}	0.91	1.98		9	0.92	1.79		10
	Fe^{3+}	0.42	0.46	-	10	0.25	0.68	-	12

Dominant portions of spectra of fresh catalysts are characteristic for spinel oxides. They exhibit the magnetic sextets of antiferromagnetic coupling, and the tetrahedral, (A) and octahedral, [B] sites can be distinguished. Iron in [B] sites exhibits larger IS and MHF values in comparison to (A) positions[18].

Most of iron in the Fe/Al_2O_3 sample is located in maghemite (γ-Fe_2O_3) structure. In correspondence, (A) and [B] sites display different IS and MHF values (Table 2). From the spectrum of the binary $Fe,Co/Al_2O_3$ catalyst incorporation of Co into the structure can be revealed: IS increases in [B] sites, the ~1:1 ratio in occupation of sites, (A)/[B], is changed to ~5:2, Co ions prefer to occupy [B] positions.

Exposure of the fresh catalysts to the reaction mixture converts the oxides to zerovalent state: the MHF values drop significantly, i.e. the antiferromagnetic oxides are converted to ferromagnetic particles.

An apparent difference between the Fe/Al_2O_3 and the $Fe,Co/Al_2O_3$ sample is clearly visible: a sextet indicating a component of a low magnetic field is present in the spectra of the single-metal Fe/Al_2O_3 catalyst in high proportion (with c.a. half of the spectral area). This low internal field (24.3 and 20.4 Tesla at 77 and 300 K, respectively) is characteristic for Θ-Fe_3C[19]. In contrast, no iron carbide is detected in the spectra of bimetallic $Fe,Co/Al_2O_3$ sample.

Inspection of spectra of the spent $Fe,Co/Al_2O_3$ catalyst reveals a further characteristic difference. The displayed metallic sextets are asymmetric (Fig. 5); they can be decomposed to two components. The magnetic field shown by the dominant component (in which c.a. half of the iron is involved) is ~34.4 Tesla. This value exceeds significantly the value characteristic for pure iron. It can only be attributed to bimetallic alloyed Fe,Co particles (since alloying with Co results in the increase of the internal magnetic field[18]). The component present in minor amount exhibits ~33.5 Tesla field, it can be attributed to metallic iron. Thus, in short, in the spectra of the spent Fe/Al_2O_3 catalyst the Θ-Fe_3C component dominates, whereas in the spectra of the $Fe,Co/Al_2O_3$ catalyst the Fe,Co bimetallic alloy is the main constituent.

A further aspect is also worth of mentioning: the overwhelming portion (≥ 80 %) of the spectra of the spent catalysts is attributed to magnetically ordered components. Considering the fact that a condition for the appearance of magnetic ordering (sextet in a Mössbauer spectrum) is a minimal particle size (6–8 nm[20]), it can also be noted that the size of the particles certainly exceeds the mentioned threshold value.

3.7 XPS spectroscopy results

Catalyst Fe/Al_2O_3

After evacuation of as received Fe/Al_2O_3, the emission of $2p_{3/2}$ appeared at 711.6 eV, while the $2p_{1/2}$ was measured at 725.1 eV. The position and energy separation are very close to that observed for FeO(OH) structure[21] and the observed broad shake-up satellite at 719.8 eV also characteristic of Fe^{3+}. Significant changes were observed when the sample was kept at 1000 K in acetylene atmosphere for 60 min. The $Fe(2p_{3/2})$ signal shifted to lower binding energy by 1.6 eV, and two satellite appeared at around 713.5 and 718.0 eV (Fig. 6A). The most important observation is that in such strong reducing atmosphere we could not detect photoemission at 707.0 eV, which is characteristic of bulk metal iron. Under this experimental condition partially oxidised iron (such as Fe_XO) should not exist on the catalyst surface. We assume that the higher binding energy indicates that the particle size is small. In the dispersed system neighbouring atoms are fewer than in bulk, therefore, screening electrons are fewer as well. As a consequence, the core-hole screening is less effective and the binding energy of the orbital shifts to higher energy. This effect could operate in the present case, too. However, the large binding energy difference could not be explained only this way, because 1000 K is high enough temperature for the agglomeration of iron particles to occur. The formation of iron-carbide (Fe_2C or Fe_3C) plays important role in the position of observed binding energy which was shown in the Mössbauer spectra as well.

Catalyst $Fe,Co/Al_2O_3$

Figure 6B shows the main photoemission signals of iron in Fe,Co bimetallic catalyst before reduction and after acetylene treatment at 300 K and 1000 K. In the unreduced samples (evacuated at 300 K and sintered at 1000 K) the peak positions were almost the same as for Fe/Al_2O_3. Acetylene adsorption at 300 K did not cause significant change. When the bimetallic catalyst was exposed to acetylene at 1000 K the $Fe(2p_{3/2})$ signal moved to higher binding energy by 0.4 eV. The same shift was observed for $(2p_{1/2})$, too. When the Fe was alone in the supported catalyst the direction of the shift was the opposite. The formation of small metallic cluster and mainly the formation of Fe_xC may explain the phenomenon. However, in this case we cannot operate with these assumptions. We attribute these changes to the formation of Fe-Co alloy. It is important to mention that similar shift was observed for $Fe,Co/TiO_2$ bimetallic catalyst after reduction[22].

In order to obtain some information about the large quantity of carbon formed on bimetallic catalyst at 1000 K, the C(1s) was also monitored by XPS. The measured 284.65 eV binding energy is higher than that of the carbidic carbon measured on Fe/Al_2O_3. This value is close to that of graphitic carbon, but it is also close to the value measured in the interaction of C_{60} fullerene and carbon nanotube with Ar ion beam[23].

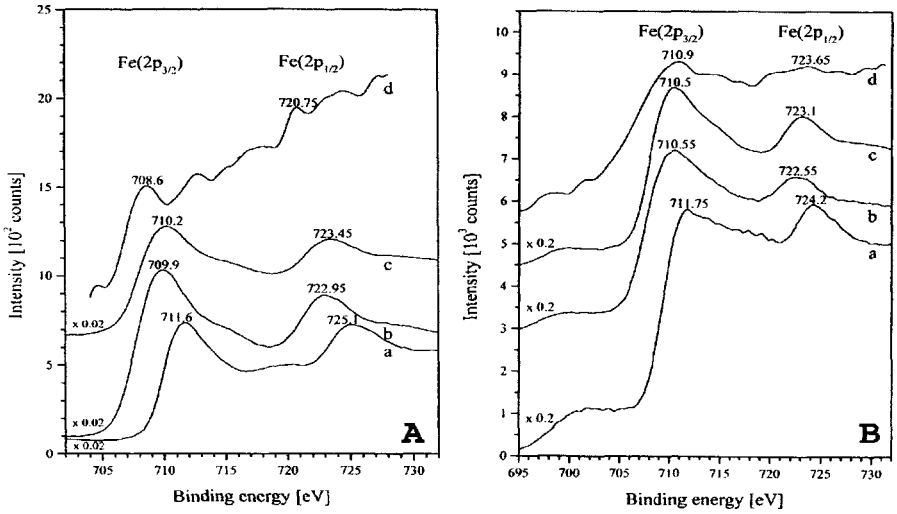

Figure 6: XPS spectra of Fe/Al_2O_3 (A) and 5%Fe+5%Co/Al_2O_3 (B) in Fe(2p) region (a) after evacuation at 300 K for 60 min, (b) after calcination at 1000 K for 20 min, (c) after 20 torr C_2H_4 adsorption at 300 K for 60 min, (d) after interaction with 20 torr C_2H_4 at 1000 K for 60 min.

4. CONCLUSION

The intimate mixing of Co and Fe took part already in the first stage: mixed Fe,Co spinel formed as it was clearly demonstrated in Mössbauer spectra. During the reaction this spinel oxide precursors were converted into catalytically active form. It was clearly demonstrated that in this step zerovalent components were formed, namely, Θ-Fe_3C on the Fe/Al_2O_3, whereas carbide formation did not take place in the Fe,Co; instead, bimetallic Fe,Co alloy was observed. In addition presence of iron can be detected in minor amounts in both the Fe and Fe,Co samples. These features are in good agreement with the literature data observed on other catalytic systems, e.g. Fischer-Tropsch reaction ($CO + H_2$); it was proven that the addition of cobalt to the iron containing catalysts suppressed the formation of iron carbides[24].

To identify a phase by XRD and by Mössbauer (for the appearance of magnetically ordered phase) a minimal size of phases is necessary. This critical size is the same range for the two methods (~6-8 nm), although it is slightly larger for XRD.

Thus, the slight discrepancy (XRD exhibits still spinel, whereas Mössbauer confirm dominating presence of Fe,Co bimetallic particles) can tentatively be explained as follows. XRD provides info on slightly larger regions than Mössbauer spectroscopy, thus, the particle size of bimetallic Fe,Co may be in the 6–12 nm range. This is in good correlation with the general inner diameter of the formed carbon nanotubes.

Summarising the results obtained in the catalytic synthesis of carbon nanotubes by Fe and Fe,Co supported on Al_2O_3, it can be stated that all the catalysts used are able to produce nanotubes, however, high activity and selectivity can be achieved using only the bimetallic sample. Mössbauer spectroscopy and XPS proved that on the bimetallic sample Fe,Co alloy was formed during the reaction and the carbon deposit was graphitic, while on the iron containing monometallic catalyst carbidic deposit was generated and carbon fibres were formed predominantly over this catalyst.

5. ACKNOWLEGEMENT

Authors thank the financial help to the European Commission and the National Science Foundation of Hungary (RTN Program, NANOCOMP network, RTN1-1999-00013, OTKA T037952). KZ acknowledges support fom the Bolyai fellowship and the Hungarian Ministry of Education (FKFP 216/2001, OTKA F038249).

REFERENCES

1. S. Iijima, "Helical microtubules of graphitic carbon", *Nature*, **354**, pp. 56-58, 1991.
2. T.W. Ebbesen, H.J. Lezec, H. Hiura, J.W. Bennett, H.F. Ghaemi, T. Thio, "Electrical conductivity of individual carbon nanotubes", *Nature*, **382**, pp. 54-56, 1996.
3. R.S. Ruoff, D.C. Lorents, "Mechanical and thermal properties of carbon nanotubes", *Carbon*, **33**, pp. 925-930, 1995.
4. A. Thess, R. Lee, P. Nikolaev, P. Dai, P. Petit, J. Robert, C. Xu, Y.H. Lee, S.G. Kim, A.G. Rinzler, D.T. Colbert, G.E. Scuseria, D. Tomanek, J.E. Fisher, R.E. Smalley, "Crystalline ropes of metallic carbon nanotubes", *Science*, **273**, pp. 483-487, 1996.
5. T.W. Ebbesen, P.M. Ajayan, "Large-scale synthesis of carbon nanotubes", *Nature*, **358**, pp. 220-222, 1992.
6. V. Ivanov, J. B.Nagy, Ph. Lambin, A. Lucas, X.B. Zhang, X.F. Zhang, D. Bernaerts, G. Van Tendeloo, S. Amelinckx, J. Van Landuyt, "The study of carbon nanotubules produced by catalytic method", *Chem.Phys.Lett.*, **223**, pp. 329-335, 1994.
7. K. Mukhopadhyay, A. Koshio, T. Sugai, N. Tanaka, H. Shinohara, Z. Kónya, J. B.Nagy, "Bulk production of quasi-aligned carbon nanotube bundles by the catalytic chemical vapour deposition (CCVD) method", *Chem.Phys.Lett.*, **303**, pp. 117-124, 1999.
8. A.M. Zhang, C. Li, S.L. Bao, Q.H. Xu, "A novel method of varying the diameter of carbon nanotubes formed on an Fe-supported Y zeolite catalyst", *Microporous and Mesoporous Materials*, **29**, pp. 383-388, 1999.
9. I. Willems, Z. Kónya, J.-F. Colomer, G. Van Tendeloo, N. Nagaraju, A. Fonseca, J. B.Nagy, "Control of the outer diameter of thin carbon nanotubes synthesized by catalytic decomposition of hydrocarbons", *Chem.Phys.Lett.*, **317**, pp. 71-76, 2000.
10. P. Coquay, R.E. Vandenberghe, E. De Grave, A. Fonsenca, P. Piedigrosso, J.B. Nagy, "X-ray diffraction and Mossbauer characterization of an Fe/SiO2 catalyst for the synthesis of carbon nanotubes", *J. Appl. Phys.*, **92**, pp. 1286-1291, 2002.
11. A.K.M. Fazle Kibria, Y.H. Mo, K.S. Nahm, "Synthesis of carbon nanotubes over nickel-iron catalysts supported on alumina under controlled conditions", *Catal. Lett.*, **71**, pp. 229-236, 2001.
12. D. Gournis, M.A. Karakassides, T. Bakas, N. Boukos, D. Petridis, "Catalytic synthesis of carbon nanotubes on clay minerals", *Carbon*, **40**, pp. 2641-2646, 2002.
13. K. Hernadi, A. Fonseca, J. B.Nagy, D. Bernaerts, A.A. Lucas, Carbon, 1996, 34, 1249; K. Hernadi, A. Fonseca, J. B.Nagy, A. Siska, I. Kiricsi, "Production of nanotubes by the catalytic decomposition of different carbon-containing compounds", *Appl. Catal. A: General*, **199**, pp. 245-255, 2000.

14. J.F. Colomer, P. Piedigrosso, I. Willems, C. Journet, C. Bernier, G. Van Tendeloo, A. Fonseca, J. B.Nagy, "Purification of catalytically produced multi-wall nanotubes", *J. Chem. Soc. Faraday T.*, **94**, pp. 3753-3758, 1998.
15. I. Vesselényi, K. Niesz, A. Siska, Z. Kónya, K. Hernádi, J. B.Nagy, I. Kiricsi, "Production of carbon nanotubes on different metal supported catalysts", *React. Kinet. Catal. Lett.*, **74**, pp. 329-336, 2001.
16. Á. Kukovecz, Z. Kónya, N. Nagaraju, I. Willems, A. Tamási, A. Fonseca, J. B.Nagy, I. Kiricsi, "Catalytic synthesis of carbon nanotubes over Co, Fe and Ni containing conventional and sol-gel silica-aluminas", *Phys. Chem. Chem. Phys.*, **2**, pp. 3071-3076, 2000.
17. Z. Kónya, "Catalytic production, purification, characterization and application of single- and multiwall carbon nanotubes", *NATO-ASI Carbon Filaments and Nanotubes: Common Origins, Differing Applications?*, L.P. Biró, C.A. Bernardo, G.G. Tibbets, Ph. Lambin, pp. 85-109, Kluwer Academic Publishers, Dordrecht, 2001.
18. R.E. Vandenberghe, E. De Grave, *Mössbauer Spectroscopy Applied to Inorganic Chemistry*, pp. 59, Kluwer Academic/Plenum Publishers, Dordrecht, 1985.
19. J.W. Niemantsverdriet, A.M. van der Kraan, W.L. van Dijk, H.S. van der Baan, "Behavior of metallic iron catalysts during Fischer-Tropsch synthesis studied with Mossbauer-spectroscopy, X-ray-diffraction, carbon content determination, and reaction kinetic measurements", *J. Phys. Chem.*, **84**, pp. 3363-3370, 1980.
20. B.S. Clausen, H. Topsoe, "Preparation and properties of small silica-supported iron catalyst particles – influence of reduction procedure", *Appl. Catal.*, **48**, pp. 327-339, 1989.
21. G.C. Allen, M.T. Curtis, A.J. Hooyer, P.M. Tucker, "X-Ray photoelectron spectroscopy of iron-oxygen systems", *J. Chem. Soc., Dalton Trans.*, pp. 1525-1530, 1974.
22. D.J. Duvenhage, N.J. Coville, "Fe:Co/TiO2 bimetallic catalysts for the Fischer-Tropsch reaction .1. Characterization and reactor studies", *Appl. Catal. A-General*, **153**, pp. 43-67, 1997.
23. Y. Zhu, T. Yi, B. Zheng, L. Cao, "The interaction of C-60 fullerene and carbon nanotube with Ar ion beam ", *Appl. Surf. Sci.*, **137**, pp. 83-90, 1999.
24. T.-A. Lin, L.H. Schwartz, J.B. Butt, "Iron alloy Fischer-Tropsch catalyst .5. FeCo on Y-zeolite", *J. Catal.*, **97**, pp. 177-187, 1986.

* konya@chem.u-szeged.hu; phone +36-62-544-619; fax +36-62-544-619